Soils and Rocks
An International Journal of Geotechnical and Geoenvironmental Engineering
www.soilsandrocks.com
ISSN 1980-9743
ISSN-e 2675-5475

Insights into drop mass systems for predicting pile compressive resistance from dynamic load test energy measurements: a case study of the Tagus River Lezíria bridge and viaducts

Jaime Santos[1,2#], Jeniffer Viegas[2]

Case Study

Keywords
Dynamic load testing
Exploratory data analysis
Supervised models
Pile foundation

Abstract

The present era is defined by the advent of big data, where large volumes of data are generated and stored daily. However, the true challenge lies in transforming this data into meaningful and actionable information. To extract insights from these vast datasets, there is a growing dependence on data-driven methods, many of which build upon traditional statistical foundations. These techniques enable the creation of models that enhance our understanding of diverse subjects and facilitate informed decision-making. This study focuses on the establishment and exploration of a database derived from dynamic load tests on piles (DLT). In DLT on piles, impact hammers are employed, characterized by their potential energy or kinetic energy just before impact. Testing on high-capacity drilled deep foundations presents several challenges, including the need for sufficient energy to mobilize compressive static resistance of the pile. The investigation delves into understanding the correlation among various DLT test variables and uncovering potential relationships using statistical models, such as linear and non-linear regression. The findings from this exploration have unveiled crucial insights, such as the influence of diameter on pile compressive resistance and stiffness and also the existence of a non-linear relationship between resistance and the maximum energy transferred to the pile.

1. Introduction

Dynamic load testing systems apply a mass to the pile head to induce load. This can be achieved either through a pile driving hammer, known as an impact driving system, or by dropping a mass, referred to as a drop mass system. Dynamic load testing can be conducted during the pile installation of precast concrete piles or steel piles (displacement piles) when driving with a hammer. Drop mass systems are employed to test cast-in-situ piles (bored piles, continuous flight auger, or other cast-in-situ piles) or testing associated with re-driving. These drop mass systems are characterized by their mass and maximum stroke (drop height), or the respective potential energy (mass × acceleration × stroke) or kinetic energy immediately just before impact.

Testing high capacity drilled deep foundations poses several challenges, one of which is determining the required energy level to mobilize the compressive static resistance of the pile. Hussein et al. (1996) conducted a wave equation analytical study for the selection of a hammer for DLT of cast-in-place shafts. The studied shafts have ranges of diameters from 750mm to 1500mm and lengths from 10 to 30 diameters. Analysis results suggest as a general guideline that the hammer weight should be about 1.5% of the pile resistance.

According to EN ISO 22477-4:2018, the mass of the drop mass should be chosen to be greater than 2% of the design compressive static resistance of the pile (where the mass of the drop mass is expressed as a weight) (EN ISO, 2018). In very hard soils, piles resting on hard bedrock, or where a pile is installed with a rock socket, drop mass weights of 1% of the required design compressive static resistance can be sufficient to mobilize pile resistance.

Ideally, the applied energy or the stroke of the drop mass should be adjusted to achieve full mobilization of the pile skin friction and tip resistance. This study focuses on the establishment and exploration of a database derived from dynamic load tests on cast-in-place foundation piles of the Tagus River Lezíria Bridge River.

[#]Corresponding author. E-mail address: jaime.santos@tecnico.ulisboa.pt
[1]Universidade de Lisboa, Instituto Superior Técnico, Instituto de Investigação e Inovação em Engenharia Civil para a Sustentabilidade, Lisboa, Portugal.
[2]TPF Consultores de Engenharia e Arquitetura S.A., Lisboa, Portugal.

Submitted on April 17, 2025; Final Acceptance on July 31, 2025; Discussion open until February 28, 2026.
Editor: Renato P. Cunha
https://doi.org/10.28927/SR.2025.006425

2. Case study

The Tagus River Lezíria Bridge comprises the north viaduct, the main bridge, and the south viaduct with a total length of about 12 km. The viaducts are supported by piles with a diameter of 1500mm, and their lengths vary between 25 and 55 meters.

The construction methodology defined to install the piles is the following (Caputo, 2009):

- Placement of a guide-steel tube with 6.00m of length;
- Driving a temporary casing with the use of vibrator down to the design depth;
- Internal cleaning of the casing up to the design depth with a hydraulic rig;
- Placement of the steel reinforcement cage;
- Cleaning of the pile tip by "air-lift";
- Pouring of the pile concrete simultaneously with the removal of the steel casing.

To validate the construction methodology and the pile design (COBA, 2005), a series of static and dynamic load tests were proposed by Instituto Superior Técnico (Santos, 2005).

Dynamic load tests were performed on 9 trial piles (6Φ800mm and 3Φ1500 mm) using specific equipment called SIPEX — Impact System for Trial Piles.

The SIPEX system employs the free fall of two 100 kN weights, each with a maximum drop height of 3 meters, capable of acting together or separately. The setup includes a guide tube, and an attached steel cap block placed over the pile. This configuration ensures a centered and vertically applied impact while protecting the pile head from potential damage (Figure 1). Although designed for testing 1500 mm diameter piles, the system can accommodate smaller diameter piles using a reducer.

Multi-blow dynamic testing technique was employed, with applied energy varying between 40 and 600 kJ (or kNm) (Paraíso & Santos, 2020).

Figure 1. SIPEX: Drop mass system 100+100 kN.

The CAPWAP (Case Pile Wave Analysis Program) method of analysis was adopted for signal matching to the dynamic measurements.

The load tests were carried out in 3 locations along the route of the viaducts, and a supplementary ground investigation campaign was defined, consisting of boreholes accompanied by SPT tests and CPTu tests. There are alluvial deposits (soft silty clay, sands) overlying gravels, boulders and the Miocene bedrock (Figure 2).

3. Methodology and results

In the current investigation, a range of variables derived from the DLT measurements are available for analysis. The CAPWAP analysis enables the evaluation of the maximum energy transferred from the hammer to the pile, the shaft and base resistance as well as the pile top displacement. Just start analyzing four independent variables: the diameter of the pile (*D*), the potential energy of the hammer or rated energy (*EP*), the maximum energy transferred from the hammer to the pile (*EMX*), the mobilized resistance (*R*), and the ratio between the mobilized resistance and the service load (*R*/*Qs*). To gain a deeper understanding of the data and the interplay among these variables, an exploratory data analysis (EDA) was undertaken. This type of analysis enables to discern the strengths of relationships between variables and to further elucidate these connections. The data underwent processing utilizing the Python open-source language, leveraging prominent libraries including Pandas, Scipy, NumPy, Seaborn, and Matplotlib.

Figure 3 showcases the correlation matrix for the aforementioned variables, while Figure 4 illustrates scatter plots for variable pairs. In this plot, piles with a diameter of 800 mm are depicted in green, and those with a 1500 mm diameter are represented in blue, complemented by variable histograms. A careful examination of these visualisations, along with the low correlation coefficients (−0.089 between diameter (*D*) and rated energy (*EP*), and 0.095 between *D* and mobilised resistance (*R*), indicates that the diameter is linearly independent of both variables, showing no meaningful linear association. As anticipated, a larger diameter would correspondingly increase resistance. Additionally, it is apparent that there exists a non-linear relationship between mobilized resistance (*R*) and maximum energy transferred from the hammer to the pile (*EMX*), with a correlation coefficient of 0.87. The influence of pile diameter is also evident, separating the data into two groups, easily discernible by colour in the scatter plot.

The efficiency of the hammer is commonly assessed by calculating the ratio between the rated energy (*EP*) and the maximum energy transferred from the hammer to the pile (*EMX*). The maximum hammer height of drop is 3m leading to a 600 kNm rated energy, displayed in Figure 5 as *EP*. It is evident that the survey was carried out for several heights (multi-blow testing technique) since the weight of the hammer was kept constant and equal to 200 kN. As

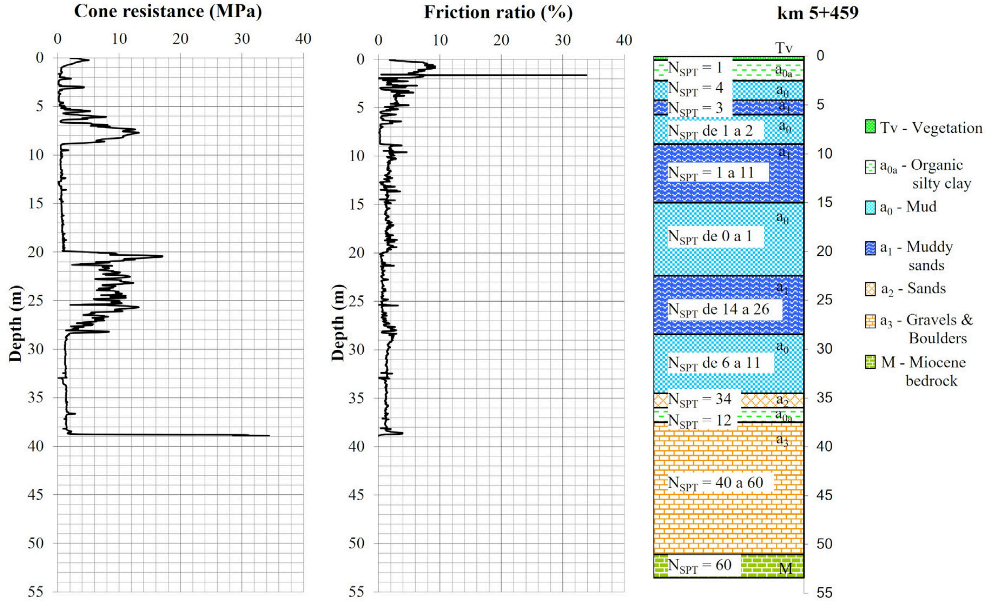

Figure 2. Typical Geological and Geotechnical Profile.

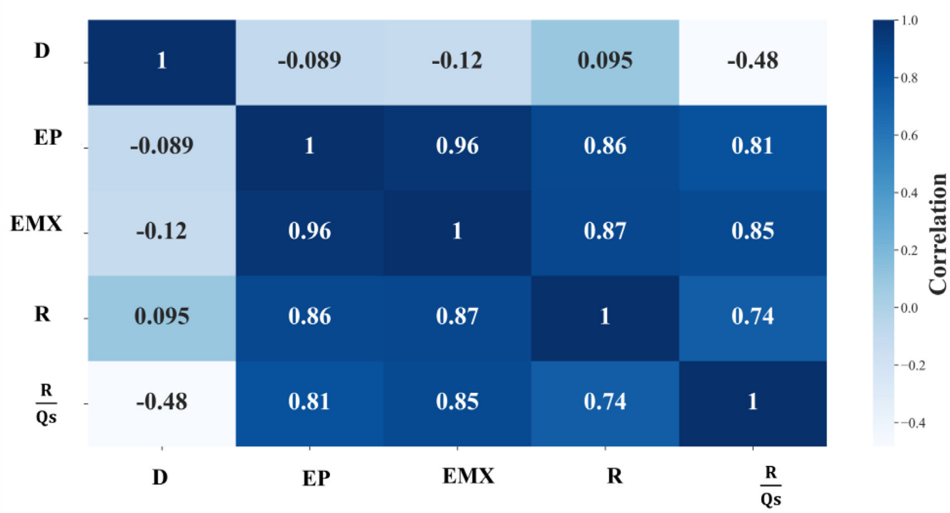

Figure 3. Correlation matrix for input variables.

depicted in Figure 5, it is evident that *EMX* is approximately 0.6 (=1/1.69) times *EP*, indicating a 40% energy loss.

In this study, the equivalent η coefficient was determined to be 0.024m, as depicted in Figure 6 (η=*EP*/*R*). This value aligns with existing literature; for instance, Paraíso & Costa (2006) reported a value of 0.033m, while Paikowsky (2004) presented a value of 0.025m. The dataset in this study displays lower dispersion, and the regression analysis yields a coefficient of determination (R^2) of 0.89, indicating a strong fit to the observed data.

It is well-known that not all energy can be transferred from the hammer to the pile. If this were possible, the coefficient η would represent the displacement associated with the plastic deformation occurring at the lateral interface of the soil-pile and at the tip (Paraíso & Santos, 2020). As indicated by EN ISO 22477-4:2018, Rausche et al. (2008) and Hussein et al. (1996), recommends that the weight of the hammer should be 1% - 2% of the desired resistance. Figure 7 elucidates this reasoning, where the ratio between the maximum energy transferred from the hammer to the pile (*EMX*) and the rated energy (*EP*) is plotted against the ratio between the hammer weight (*W*) and the mobilized resistance (*R*).

It is evident that for the 800 mm diameter, the loss of energy is minimized when the weight/resistance ratio falls between 1% - 2% (shaded area in Figure 7), more

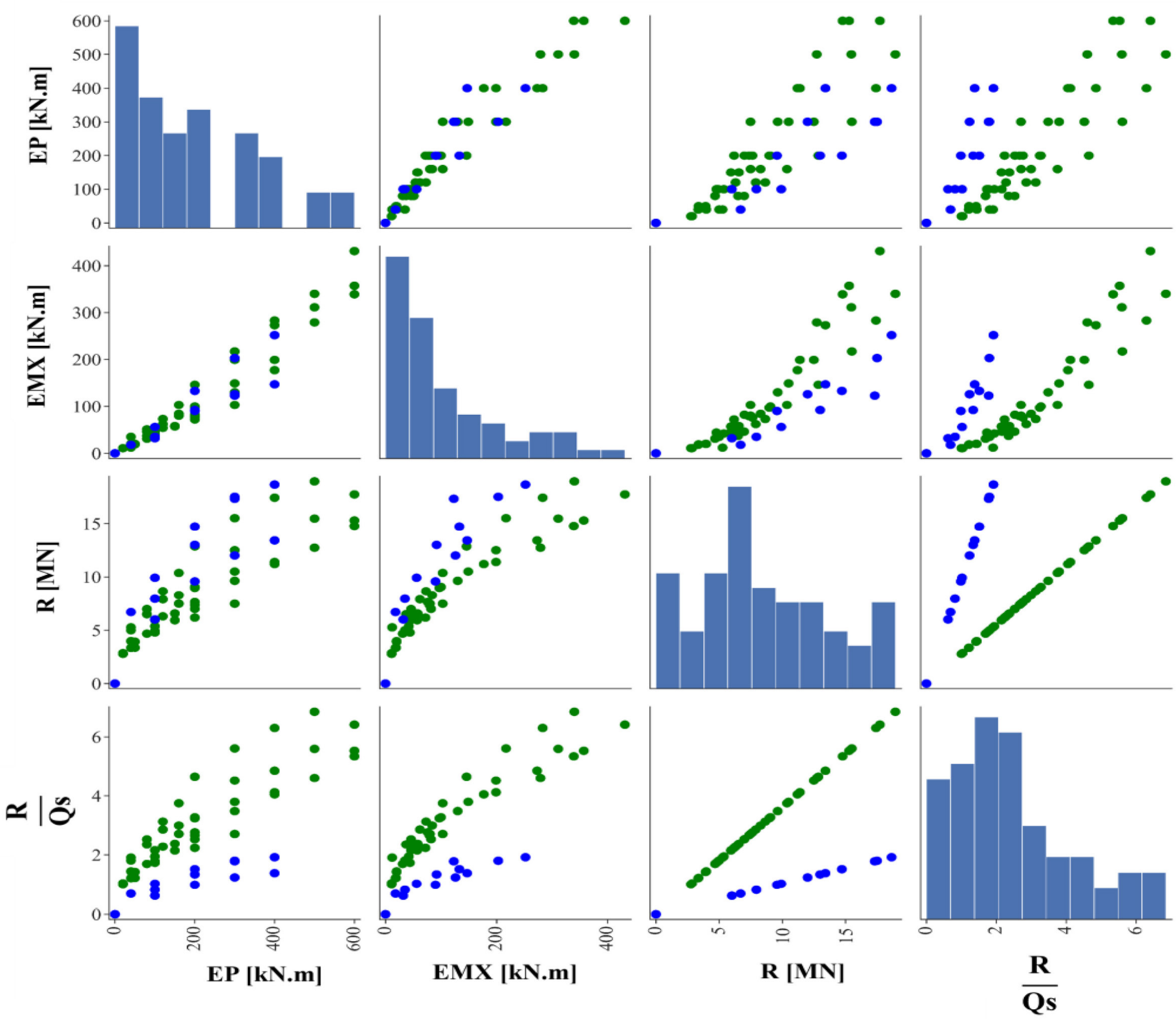

Figure 4. Scatterplot matrix depicting the relationships among the investigated variables. The green color represents the piles with 800 mm diameter and the blue the ones with 1500 mm.

precisely between 1% – 1.3%, in this study, for the blows that mobilized the maximum resistance. However, for the 1500 mm diameter, three points deviate from the trend, and within this interval, they still exhibit a lower energy ratio, approximately 40%. The efficiency of the hammer ranges from 30% to 87.5%, with a mean of 50.9%.

Upon closer examination of the *EMX* distribution for both diameters, as illustrated in Figure 8, it becomes evident that both distributions exhibit comparable means. However, the 1500 mm diameter piles display higher dispersion due to the limited number of samples, which could justify this misalignment with the trend in Figure 7.

While the presented results are intriguing, the aim is to offer practical insights beneficial for designers. A key interest lies in determining the hammer parameters required to attain a specific resistance. In order to address this, a non-linear regression analysis was conducted between *EMX* and *R*, as presented in Figure 9. Various functions underwent testing, and the one presented yielded the lowest Root Mean Square Error (*RMSE*).

Notably, the equation for the 800 mm diameter is approximately double that of the equation for the 1500 mm diameter, revealing the influence of the diameter on the equation. It is important to emphasize that the regression was constrained to pass through the origin, reinforcing the expectation of zero energy being applied at zero resistance. This graphical representation underscores that the requisite energy for achieving a given resistance is consistently lower for the larger diameter, thereby justifying an increased cost in pile designs with a corresponding reduction in associated

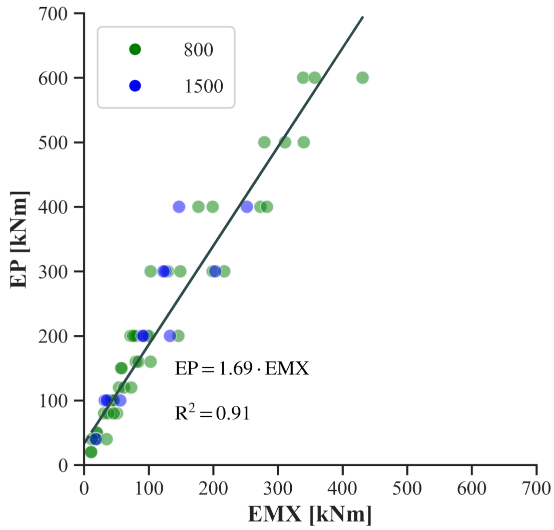

Figure 5. Relationship between the rated energy (*EP*) and the maximum energy transferred from the hammer to the pile (*EMX*), for both diameters 800mm (green) and 1500 mm (blue).

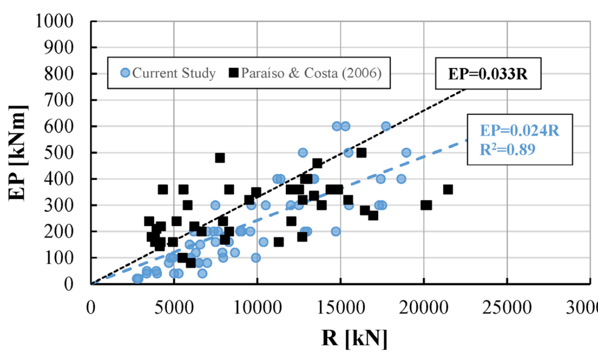

Figure 6. Comparison between the dataset of the current study (in blue) and the one presented in Paraíso & Costa (2006) (in black).

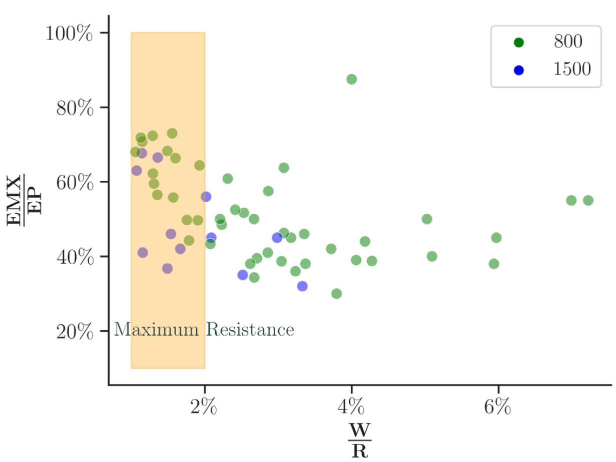

Figure 7. Relationship between the ratio of maximum energy transferred from the hammer to the pile (*EMX*) to rated energy (*EP*) and the ratio of hammer weight (*W*) to resistance (*R*). The orange area highlights the zone where the maximum resistance is mobilized.

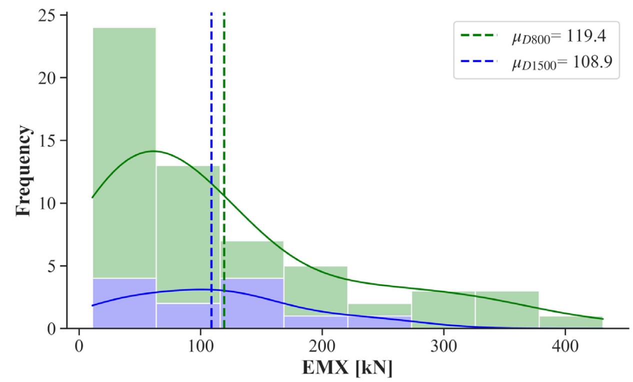

Figure 8. Distribution of the maximum energy transferred from the hammer to the pile (*EMX*) for both diameters. The green color represents the 800 mm diameter, while the blue represents the 1500mm. The dashed lines are the mean of each distribution.

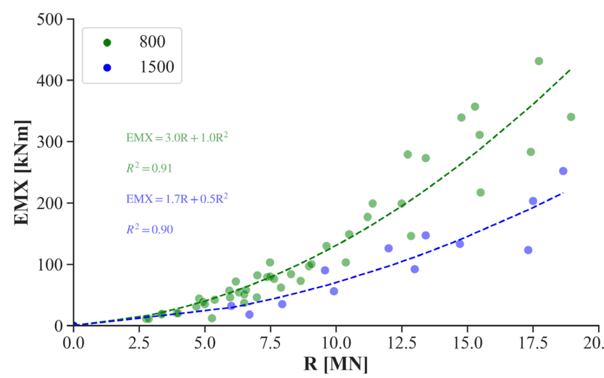

Figure 9. Non-linear relationship between the maximum energy transferred from the hammer to the pile (*EMX*) and the mobilized resistance (*R*). The green color represents piles with a 800 mm diameter, while the blue represents those with a 1500mm diameter.

equipment, or where the applied energy should be limited due to displacement issues.

Furthermore, three more variables are added to the analysis to gain a deeper understanding of our data (Figure 10): the mobilized lateral resistance (*Rs*), the mobilized base resistance (*Rb*), and the maximum pile top displacement (*DMX*).

Upon analyzing the decomposition of the total mobilized resistance (*R*) into its lateral component (*Rs*) and base component (*Rb*) alongside the maximum energy transferred from the hammer to the pile (*EMX*), it becomes evident that the nonlinearity in the *R-EMX* relationship primarily arises from the dominant influence of the lateral component (*Rs*), as illustrated in Figure 10. This becomes evident when the lateral resistance is approaching the ultimate value. The *Rb-EMX* relationship appears more linear, whereas the *Rs-EMX* curve exhibits nonlinearity. Furthermore, in the *Rb-EMX* plot, the influence of the pile diameter is significant, as it distinctly separates the data into two groups, highlighting

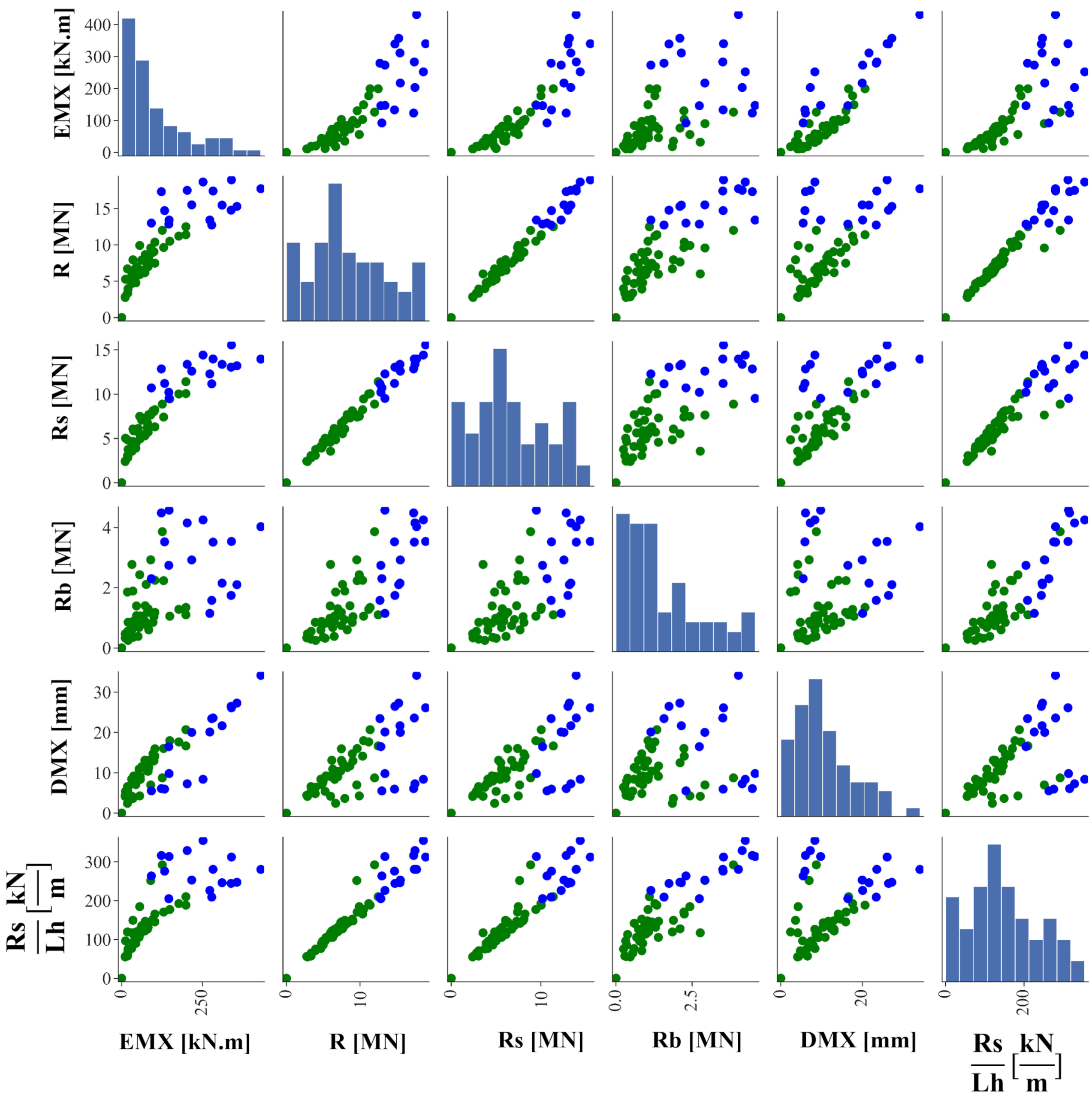

Figure 10. Scatterplot matrix depicting the relationships between mobilized resistance (*R*) and its components (*Rs*, *Rb*), the maximum pile top displacement (*DMX*), and the maximum energy transferred to the pile (*EMX*). The green color represents the piles with 800 mm diameter and the blue the ones with 1500 mm.

the influence of pile diameter. In contrast, the *Rs-EMX* plot shows much lower dispersion, suggesting less influence of the diameter. These trends appear to be logical since the base resistance varies with the square of the diameter, while the lateral resistance varies linearly with the diameter of the pile.

To gain a deeper understanding of these relationships, a regression analysis was conducted, with the variables grouped by pile diameter and linked to their corresponding piles (Figure 11). This approach allows us to assess the influence of spatial variation and lithology on the variables. The dynamic pile load tests were carried out in 3 locations with distances of approximately 3 km between them.

Figure 11 summarizes the relationships involved with the maximum energy transferred to the pile (*EMX*). The green lines and crosses denote piles with an 800 mm diameter, whereas the blue lines and circles represent piles with a 1500 mm diameter.

The regression results in Figure 11 demonstrate a strong fit for *R*, *Rs*, and *DMX*. In contrast, *Rb* exhibits considerable

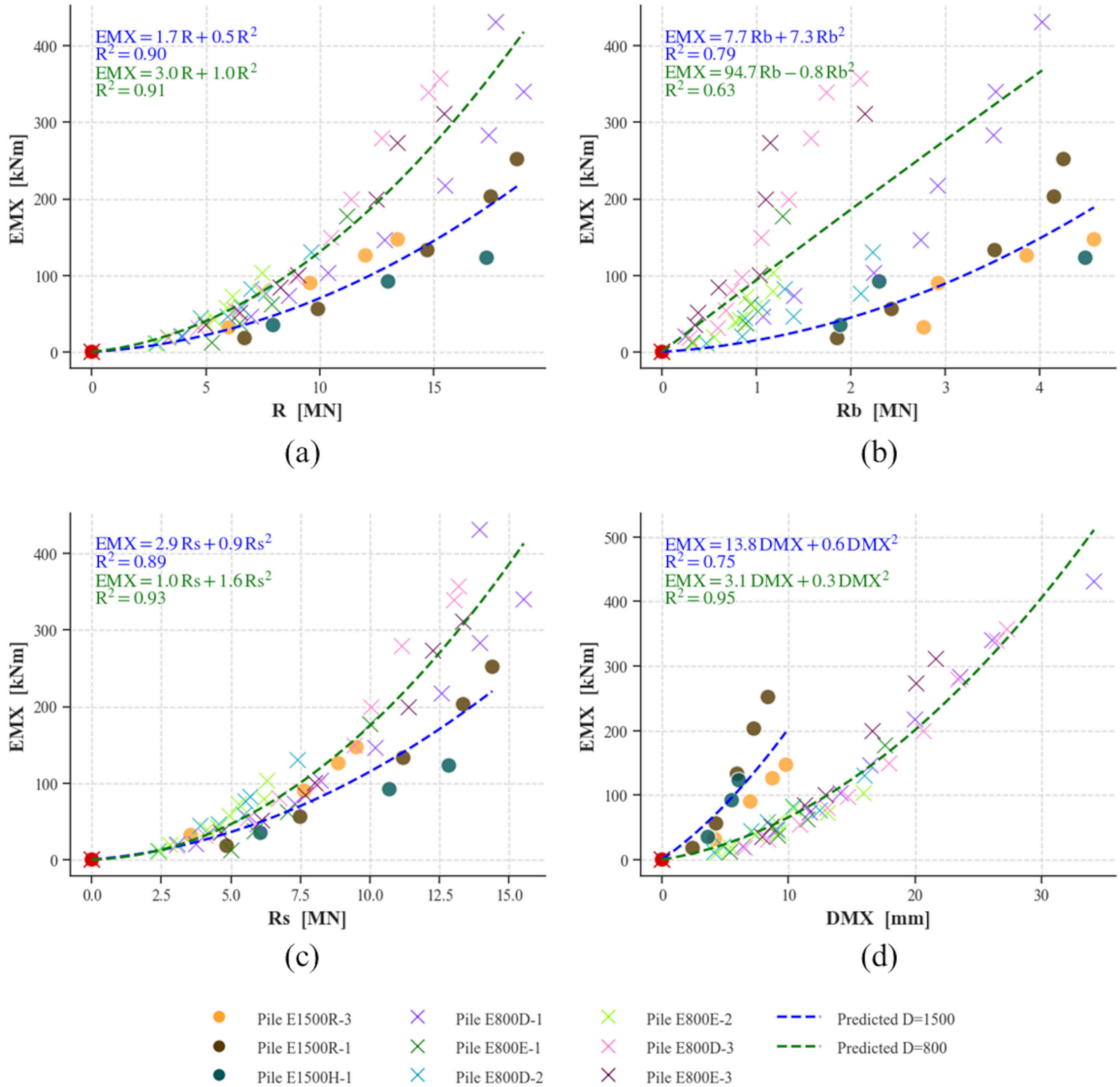

Figure 11. Non-linear relationship between the maximum energy transferred to the pile (*EMX*) and: (a) the total mobilized resistance (*R*), (b) the base resistance (*Rb*), (c) the lateral resistance (*Rs*), (d) the maximum pile top displacement (*DMX*).

scatter, largely attributable to variations in the embedding soil material, which ranges from Miocene deposits to bouldery formations. Additionally, installation effects during construction may influence the observed behavior. Besides, the *Rb-EMX* relationship appears quite linear, so it is not possible to derive any considerations about the ultimate base resistance. It is also important to highlight that the lateral resistance is dominant in all piles tested, representing more than 83% of the total resistance. The *Rs-EMX* curve exhibits nonlinearity and physically should converge to asymptotic values that represent the ultimate lateral resistance.

For reasons of uniformity and simplicity in data processing, polynomial regression functions were used in the previous figures. While these functions offer flexibility in modeling nonlinear relationships, they lack asymptotic values, which can be a limitation when modeling physical problems. For such cases, hyperbolic functions are more suitable, as they can easily handle asymptotic behavior. For this reason, the lateral resistance divided by the total length *Rs*/*L* is plotted against *EMX* and fitted using hyperbolic functions in Figure 12.

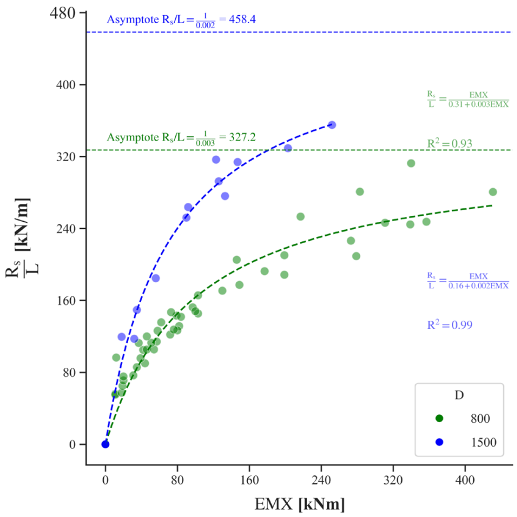

Figure 12. The relationship between the lateral resistance per unit length (*Rs*/*L*) and the maximum energy transferred to the pile (*EMX*).

The regression results shown in Figure 12 indicate a strong fit for both pile diameters ($R^2 \geq 0.93$). The asymptotic values of the regression curves represent the ultimate lateral resistance per unit length. The ratio 458.4 / 327.2 ≈ 1.4 is relatively close to the ratio of the pile diameters, 1500 / 800 ≈ 1.87. However, the 1500 mm diameter reaction piles are slightly shorter and have a reduced embedded length within the Miocene deposits or bouldery formations. This difference in geometry and soil interaction helps explain why, on average, the ultimate lateral resistance per unit length is lower for the larger-diameter piles.

Figure 13, similar to Figure 11, illustrates the relationship between maximum pile top displacement and the mobilized resistance components. The data follows a linear regression trend, confirming that piles with larger diameters experience significantly less displacement, as previously mentioned. This linear behavior arises because the *DMX* value represents the maximum displacement associated with a given blow and

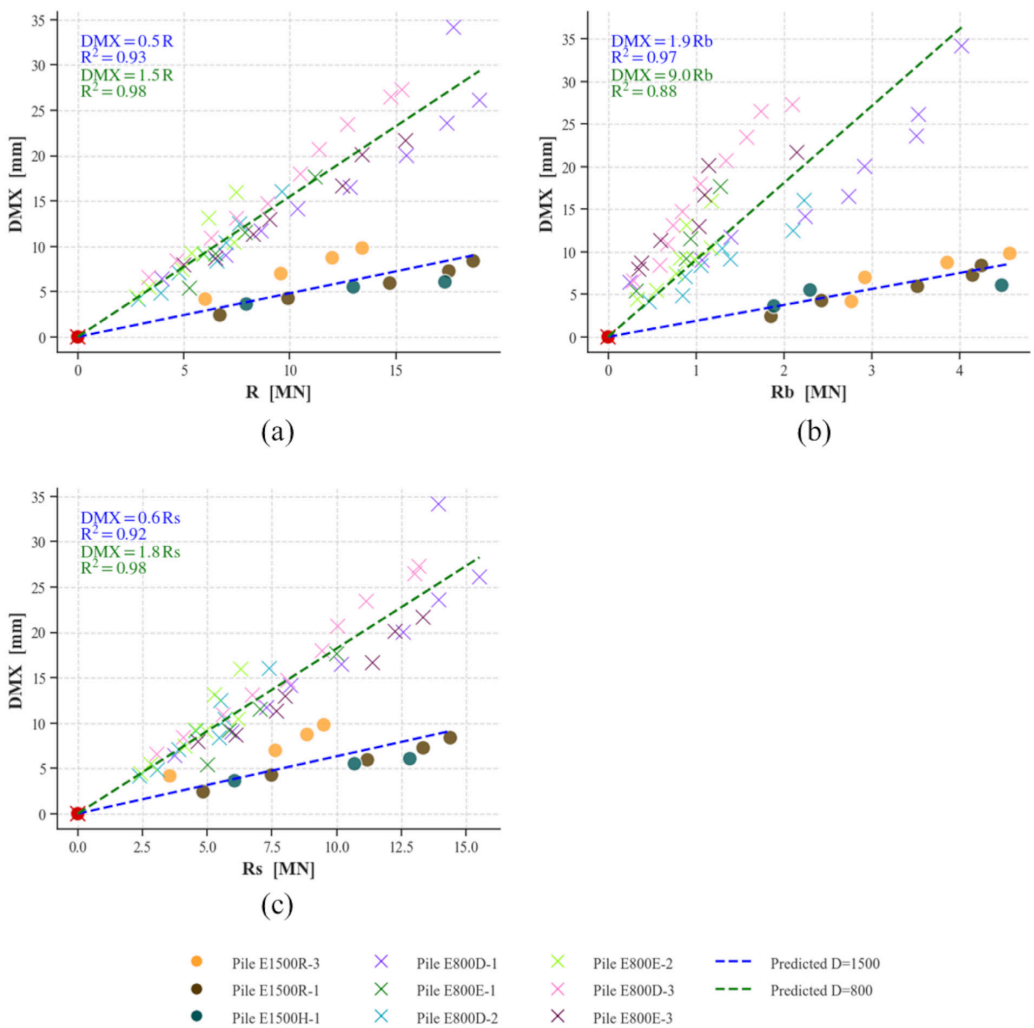

Figure 13. Linear relationship between the maximum displacement (*DMX*) and: (a) the total mobilized resistance (*R*), (b) the base resistance (*Rb*), (c) the lateral resistance (*Rs*).

does not account for the permanent displacement accumulated from previous blows. In this sense, it reflects the quasi-elastic response of the resistance during successive load-unload cycles, as observed in dynamic load tests involving multiple blows of increasing energy.

Examining the relationship between the pile's top maximum displacement (*DMX*) and its components, *Rb* and *Rs*, it is possible to observe a clear distinction between different diameters. Specifically, for the same resistance, piles with smaller diameters (green) exhibit three times greater displacement, likely due to movement along the soil–pile lateral interface. This interface displacement is governed by the thickness of the soil shear band and the relative displacement between the soil and the pile. In this case study, the soil type is essentially the same for all tested piles; however, the soil–pile relative displacement is influenced by pile shortening, i.e., by compressive stress. The ratio of the cross-sectional areas is approximately 3 (1500^2 / 800^2 = 3.5), which supports the trend observed in the data.

4. Conclusion

In this comprehensive investigation, variables obtained from the Dynamic Load Test (DLT) were examined, including the maximum potential energy of the hammer (rated energy, *EP*), the maximum energy transferred from the hammer to the pile (*EMX*), and the mobilized resistance (*R*). The interrelationships between these variables were also explored in detail. Practical implications for predicting pile compressive resistance from dynamic load test energy measurements are underscored and materialized through regression equations. The results obtained not only align with current literature but also pave the way for valuable insights. Specifically, the formulated equations for predicting pile compressive resistance demonstrate excellent agreement with the dataset, boasting a coefficient of determination (R^2) around 0.9 (Figures 6 and 9). This high level of correlation underscores the robustness and reliability of the equations in capturing the dynamics of the system.

In pursuit of a more comprehensive understanding, examining the relationships with additional variables - such as lateral resistance, tip resistance, and the maximum pile top displacement - separately, could significantly enhance the accuracy and applicability of the derived equations. For this case study, the lateral resistance is dominant in all piles tested. The hyperbolic functions used to predict the lateral resistance per unit length demonstrate an excellent fit, with a coefficient of determination greater than or equal to 0.93 (Figure 12). Additionally, the relationships between the lateral resistance and the pile top displacement offer valuable insights into the stiffness behavior of the soil–pile system (Figure 13).

This study stands as a significant contribution to the field, providing new practical tools for engineers and designers involved in pile-related projects, in particular at the Tagus River zone in Lisbon, potentially contributing to cost and time savings by reducing the need for extensive in-situ pile testing.

This study also represents the initial step toward developing machine learning approaches — the exploratory data analysis phase. The available features were examined, their interrelationships assessed, and the most relevant variables for future predictive modeling identified. The next step involves expanding the dataset by incorporating additional variables, such as results from cone penetration tests (CPTu) and standard penetration tests (SPT), to further enhance the understanding of pile behavior with integrated physics knowledge. A key challenge will consist of the use of a dataset of sufficient size and quality to ensure robust training and validation of the model.

Acknowledgements

The authors would like to acknowledge Brisa – Autoestradas de Portugal S.A. for authorizing the publication of the data presented in this work. Appreciation is also extended to the TACE construction consortium, composed of MSF, Construtora do Tâmega, Lena Construções, Novopca, Bento Pedroso Construções, and Zagope, for their valuable support of the pile testing program. The authors further wish to thank Geomec for their valuable assistance in conducting the dynamic pile load tests, including the interpretation of CAPWAP analyses.

Declaration of interest

The authors have no conflicts of interest to declare. All co-authors have observed and affirmed the contents of the paper and there is no financial interest to report.

Authors' contributions

Jaime Santos: conceptualization, methodology, data interpretation, writing – original draft. Jeniffer Viegas: formal analysis, software, methodology, writing – original draft.

Data availability

All data produced or examined in the course of the current study are included in this article.

Declaration of use of generative artificial intelligence

This work was prepared with the assistance of generative artificial intelligence (GenAI) OpenAI's ChatGPT with the aim of enhancing readability and refining language. The entire process of using this tool was supervised, reviewed and when necessary edited by the authors. The authors assume full responsibility for the content of the publication that involved the aid of GenAI.

List of symbols and abbreviations

a_0	Alluvial mud
a_{0a}	Alluvial Organic silty clay
a_1	Alluvial muddy sands
a_2	Alluvial sands
a_3	Alluvial gravels & boulders
CAPWAP	Case Pile Wave Analysis Program
CPTu	Cone penetration test
D	Pile diameter
DLT	Dynamic load test
DMX	Maximum pile top displacement
EDA	Exploratory data analysis
EMX	Maximum energy transferred from the hammer to the pile
EP	Potential energy of the hammer or rated energy
L	Pile length
M	Miocene bedrock
N_{SPT}	Number of blows in SPT tests
Qs	Pile service load
R	Pile (mobilized) total resistance
R^2	Coefficient of determination
Rb	Pile (mobilized) base resistance
$RMSE$	Root mean square error
Rs	Pile (mobilized) lateral resistance
SIPEX	Impact System for Trial Piles
SPT	Standard penetration test
Tv	Vegetation
W	Hammer weight
η	Ratio between the potential energy and he mobilized pile resistance
μ_{D1500}	Mean EMX for piles with 1500 mm diameter
μ_{D800}	Mean EMX for piles with 800 mm diameter
Φ	Pile diameter

References

Caputo, A. (2009). Instrumented large diameter bored piles. In W.F. van Impe & W. Haegeman (Eds.), *Deep foundations on bored and auger piles* (pp. 213-227). London: Taylor & Francis Group.

Consultores de Engenharia e Ambiente S.A. – COBA. PC&A. Civilser. Arcadis. (2005). *Geological and geotechnical study: description of the solution. Final design of the bridge crossing Tagus river and access viaducts.* Lisboa.

EN ISO 22477-4. (2018). *Geotechnical investigation and testing: testing of geotechnical structures: testing of piles: dynamic load testing.* International Organization for Standardization, Geneva.

Hussein, M., Rauche, F., & Linkins, G. (1996). Selection of a hammer for high strain dynamic testing of cast in place shafts. In *Proceedings of the 5th International Conference on the Application of Stress-Wave Theory to Piles* (pp. 759-772), Orlando, Florida, USA. UGent.

Paikowsky, S.G. (2004). Drop weight dynamic testing of drilled deep foundations. In *Proceedings of the 7th International Conference on the Application of Stress-Wave Theory to Piles* (pp. 13-81), Kuala Lumpur, Malaysia. GRL Engineers, Inc.

Paraíso, S.C., & Santos, J.A. (2020). Ensaio de carregamento dinâmico de energia crescente em estacas de elevada capacidade resistente. *Revista Geotecnia*, *50*, 7-25. http://doi.org/10.24849/j.geot.2020.150.02.

Paraíso, S.C., & Costa, C.M.C. (2006). Análise do desempenho de martelo hidráulico autopropulsor testando estacas de alta capacidade de carga. In *Anais do COBRAMSEG* (pp. 1079-1084), Curitiba, PR. São Paulo: ABMS.

Rausche, F., Nagy, M., & Likins, G. (2008). Mastering the art of pile testing. In *Proceedings of the 8th International Conference on the Application of Stress-Wave Theory to Piles* (pp. 19-32), Lisbon, Portugal. Lisboa: Instituto Superior Técnico.

Santos, J.A. (2005). *A10-Bucelas/Carregado/IC3 Highway, Carregado subsection (A1) Benavente: Tagus river crossing in Carregado: load tests on trial piles: analysis report*. Lisboa: ICIST, Instituto Superior Técnico.